EPR, UV-visible and Near infrared spectroscopic characterization of dolomite

S. Lakshmi Reddy[1*],G.Sowjanya[1], N.C.G.Reddy[2], G.Siva Reddy[2], B.J.Reddy[3] & R.L.Frost[3]

1. Dept. of Physics, S.V.D. College, Kadapa 516 003, India.
2. Dept.of chemistry, Yogi Vemana University, Kadapa 516 003, India.
3. Inorganic Materials Research Program, Queensland University of Technology, 2 George Street, Brisbane, GPO Box 2434, Queensland 4001, Australia

*Corresponding author email: slreddy_in@yahoo.com

Key words: Dolomite mineral, optical absorption spectrum, EPR spectrum, Fe(III) , Mn(II), near-infrared spectroscopy.

Abstract

Dolomite mineral samples having white and light green colours of Indian origin have been characterized by EPR, optical and NIR spectroscopy. The optical spectrum exhibits a number of electronic bands due to presence of Fe(III) ions in the mineral. From EPR studies, the parameters of g for Fe(III) and g, A and D for Mn(II) are evaluated and the data confirm that the ions are in distorted octahedron. Optical absorption studies reveal that Fe(III) is in distorted octahedron. The bands in NIR spectra are due to the overtones and combinations of water molecules. Thus EPR and optical absorption spectral studies have proven useful for the study of the chemistry of dolomite.

1. Introduction

Carbonate minerals in various forms such as limestone, dolomite, calcite etc., constitute the earth's largest CO_2 resource. The dolomite group of minerals have the general formula $A^{++}B^{++}(CO_3)_2$. When large amount of iron is present, the mineral ankerite forms and when excess manganese is present the mineral kuntnohorite forms instead of dolomite. All these minerals have the same internal structure but differ chemically from each other [1]. This group of minerals is classified [2] into several types as given below:

Ankerite	$Ca(Fe,Mg,Mn)(CO_3)_2$
Benstonite	$(Ba,Sr)_6(Ca,Mn, Mg)_6(CO_3)_{12}$
Dolomite	$CaMg(CO_3)_2$
Huntite	$CaMg_3(CO_3)_4$
Kuntnohorite	$Ca(Mn,Mg,Fe)(CO_3)_2$
Minrecordite	$(Ca,Zn)(CO_3)_2$
Norsethite	$BaMg(CO_3)_2$

In the above group of minerals, Mg(II) can be replaced by ferrous iron and manganese. In dolomites the Mn(II) ion is a natural substitutional impurity at the sites of both Ca(II) and Mg(II) ions. Composition of low-Mn ankerite generally approached the formula $CaMg(CO_3)_2$ - $CaFe(CO_3)_2$. [3]. This group of minerals has the wide useful applications especially as fillers some of which are given below:

- in cement paints, exterior paints, primers, putties, powder coatings and industrial finishes.
- in PVC footwear, PVC pipes, cables and others.
- in paper to give smoothness and gloss
- in adhesives and carpet backing and
- in toothpaste, cosmetic and soap industry.

Dolomites are iso-structural having space group R_3. Dolomite structure reveals that there are two distinct cation sites denoted by A and B [4]. These both sites form nearly regular octahedra in which each corner of an octahedron is oxygen from a different CO_3 group. The site A is occupied by Ca and the B site is occupied by Mg in the ideally ordered case with layers of Ca octahedron alternating with layers of (Mg,Fe,Mn) octahedron. The octahedra are linked by sharing corners simultaneously with octahedra of the opposite kind with CO_3 groups [4]. The two octahedra in dolomite are trigonally distorted by elongation along the three fold axis. The larger A octahedron is always slightly more distorted than that in B [4,5]. Detailed spectral studies have been reported on dolomite-ankerite series but not on dolomite of Indian origin [3,6-8]. Several studies have been made on natural dolomites from different origins using EPR studies [9-11]. However few EPR studies have been done which could identify paramagnetic radicals in dolomites around g = 2.0023 [11]. However complete interpretation of the EPR spectra of dolomites is not available. Hence, optical absorption and EPR studies on some natural carbonate minerals have been made [12].

Transition metal ions such as Fe(III),Mn(II) and V(IV) display a rich coordination in minerals. For the identification and characterization of these metal ions in natural systems, electron paramagnetic resonance has been found to be the most powerful analytical technique. In India, Kadapa Basin endowed with rich mineral resources. In this paper, we report the EPR and optical absorption spectral studies of dolomites obtained from Vempalli Mandal of Kadapa district, Andhra Pradesh, India.

Theory

Several EPR parameters i.e., g, A, D, and E are used while interpreting EPR data. The g parameter is a measure of the coupling between the unpaired electron's spin angular momentum (S) with its orbital angular momentum (L) [13].

The unpaired electron interacts (couples) with the nuclear spin (I) to form a ($2I + 1$) line hyperfine structure centered on g and spaced with the distance quantified by the hyperfine coupling parameter A. The coupling between the nuclear and electron spins becomes stronger as the A parameter becomes larger. The combination of g and A parameters can be utilized to differentiate between electron environments of Fe^{3+} and

Mn^{2+} ions. The EPR zero field splitting (ZFS) parameters *D* and *E* measure the deviation of the ion crystal field from ideal tetrahedral or octahedral symmetries and they apply to ions with more than one unpaired electron, e.g., low field Fe^{3+} and Mn^{2+}. However, the broad nature of EPR spectra of Fe^{3+} makes the determination of *D* and *E* difficult [14].

Mn(II), being a d^5 ion, has total spin S = 5/2. This state splits into three Kramers' doublets, ±5/2>, ±3/2>and ±1/2> separated by 4D and 2D respectively. Where, D is the zero-field splitting parameter. The deviation from axial symmetry leads to a term, known as, E, in the spin Hamiltonian. The value of E can be easily calculated from single crystal measurements. A non-zero value of E results in making the spectrum unsymmetrical about the central sextet.

RESULTS AND DISCUSSION

Total Chemical Analyses

Dolomite minerals examined in this study are ankerite and dolomite. Elemental compositions of metal are listed in Table -1 [15-17].

EPR spectral analysis

EPR spectrum of the dolomite mineral samples recorded at room temperature is given in Fig. 1 (a) and 1(b). The overall EPR spectral features are similar in both the dolomites. It is well known that the EPR studies of transition metal ion Mn(II) is easily observed at room temperature, even if present in minute levels, compared to other ions. Both the spectra [Fig. 1 (a) and 1(b)] clearly indicate the presence of Mn(II) in the sample. An expanded version of central sextet is shown in Fig. 2 (a) & 2 (b).

Fig. 1 (a) and 1(b) contains a strong sextet at the centre of the spectrum corresponding to the electron spin transition +1/2> to -1/2>. Generally, in most of the cases, the powder spectrum is characterized by a sextet, corresponding to this transition. The other four transitions, corresponding to ±5/2> ↔ ±3/2> and ±3/2>↔ ±1/2> are not seen due to their high anisotropy in D. If E ≠ 0, the EPR spectrum will not be symmetrical about the central sextet. The expanded version of the powder spectrum [Fig. 2 (a) & 2(b)] of both dolomite mineral samples indicate the presence of at least four types of Mn(II) impurities in the mineral. The sixth manganese hyperfine resonance clearly contains two lines (marked by a and b). This is also followed by two more sets of weak lines (marked by * and **) on either side of the intense Mn(II) signals as shown in Fig.2 (a) & 2 (b). This is same in both the samples. This is due to the presence of Mn(II) ions in a low symmetry environment [18] **.** The EPR line intensity of Mn(II) hyperfine lines observed in green dolomite is more intense, when compared to that in the white dolomite mineral. This indicates clearly that the concentration of Mn(II) ions in green dolomite sample is more than that in the white dolomite. Even when viewed with a naked eye, the sample is pale greenish pink in colour indicating the substitution of manganese ion in larger concentration in this mineral.

The observed EPR spectrum can be explained by the spin-Hamiltonian of the form [19].

$$\mathcal{H} = \beta BgS + D\{S_Z^2 - \frac{1}{3}S(S+I)\} + SAI$$

Here the first term represents the electron-Zeeman interaction. The second term represents the zero field contribution and the third term represents the nuclear-Zeeman interaction. The extra set of resonances in between the main sextet is due to the forbidden transitions. From the forbidden doublet lines, the Zero field splitting parameter, D, has been calculated using the formula [20, 21].

$$\Delta H = \left(\frac{2D^2}{H_m}\right)\left[\frac{1+16(H_m - 8Am)^2}{9H_i H_m - 64Am}\right]$$

$$\text{Here } H_m = H_o - Am - \frac{[I(I+1) - m^2]A^2}{2H_o}$$

From the powder spectrum of the mineral, the following parameters have been calculated:

White dolomite g = 1.992 ± 0.015, A = 9.15 ± 0.43 mT and D = 34.45 ± 0.36 mT.
Green dolomite g = 1.993 ± 0.017, A = 9.35 ± 0.43 mT and D = 34.25 ± 0.35 mT.

The observed g, A and D values are comparable with other similar systems and agree well within the experimental error [8,22-25].The large value of D indicates a considerable amount of distortion around the central metal ion. As EPR is highly sensitive to Mn(II) impurity, four such sites have been noticed in the EPR spectrum. A close look at the EPR spectrum indicates a non-zero value for E, which is very difficult to estimate from powder spectrum. A close look at the centre of the EPR spectrum indicates a broad line underneath the Mn(II) sextet. This can be attributed to the iron impurity in the sample. Generally, Fe(III) and Fe(II) impurities will give rise to a broad line around with a g value of 2. No extra information can be obtained from the powder spectrum recorded at room temperature and low temperature except that iron is present as an impurity. Even though the percentage of iron is more than that of manganese, its intensity is relatively smaller compared to the signals obtained from the manganese impurity. The EPR spectrum of white dolomite exhibits a broad resonance centered when g is 4.20 similarly a weak resonance is observed when g is 4.34 in the case of green dolomite. Those are attributed to the presence of isolated Fe(III) ions incorporated as an impurity in the mineral..

The hyperfine constant 'A' value provides a qualitative measure of the ionic nature of bonding with Mn(II) ion. The percentage of covalency of Mn-ligand bond in green dolomite has been calculated using 'A' (9.35 mT) value obtained from the EPR spectrum and Matumura's plot [26]. It corresponds to an ionicity of 94%, where as in the case of white dolomite, 'A' with a value of 9.15 mT gives an ionicity of 91%. Also the approximate value of hyperfine constant (A) is calculated for both dolomites by using covalency (C) using the equations [27, 28]

$$A_{iso} = (2.04C - 104.5)\ 10^{-4}\ cm^{-1}.$$

The value obtained is 92x 10^{-4} cm^{-1} for green dolomite and whereas for the white dolomite it is 91x 10^{-4} cm^{-1} . This calculated value agrees well with the observed hyperfine constant for both the samples indicating ionic character for Mn-O bond in the mineral under study. The number of ligands around Mn(II) ion is estimated using the covalency [27] equation for C

$$C = \frac{1}{n}\left[1 - 0.16\left(X_p - X_q\right) - 0.035\left(X_p - X_q\right)^2\right]$$

Here X_P and X_q represent electronagativities of metal and ligand. Assuming $X_p = X_{Mn} =$ 1.4 and $X_q = X_O = 3.5$, the number of ligands (n) obtained are 20. This suggests that Mn(II) may be surrounded by four CO_3^{2-} and two oxygens. Further the g value for the hyperfine splitting is indicative of the nature of bonding. If the g value shows negative shift with respect to free electron g value of 2.0023, the bonding is ionic and conversely, if the shift is positive, the bonding is more covalent in nature [29]. In the present work, from the observed negative values of 0.0103 for white dolomite and that of -0.0093 for green dolomite, it is apparent that the Mn(II) is in an ionic environment. EPR spectrum of white dolomite [Fig. 2 (b)] reveals that in between first and second manganese hyperfine resonance lines a very weak sharp peak at (319.2 mT) having a g value 2.1019 is observed. This can be ascribed to a radical such as CO_3^{2-} or NO_3^{2-}. The absence of any super hyperfine structure in the radical suggests that the radical may be CO_3^{2-} [11]

Optical absorption spectral analysis

Ferric iron, Fe(III), has the electronic configuration Ar ($3d^5$) with a half filled d-shell having one unpaired electron in each of the orbital. Hence ground state configuration is $t_{2g}^3\ e_g^2$. The free ion levels of Fe(III), in the order of increase in energy are ^6S, ^4G, ^4P, ^4D, ^4F. The energy levels for Fe(III) in an octahedral environment are $^6A_{1g}(^6S)$, $^4T_{1g}(^4G)$, $^4T_{2g}(^4G)$, $^4A_{1g}(G)$- $^4E_g(^4G)$, $^4T_{2g}(^4D)$ and $^4E_g(^4D)$. The $^4A_{1g}(G)$- $^4E_g(^4G)$ and ^4E_g (^4D) levels have relatively less influence compared to other levels by crystal field. It means that the relative sharp levels can be expected in the absorption spectrum which is the criterion for assignment of levels for Fe(III) ion. Since all the excited states of Fe(III) ion will be either quartets or doublets, the optical absorption spectra of Fe(III) ions will have only spin forbidden d-d transitions. These occur from the ground state $^6A_{1g}(S)$ to the excited states $^4T_{1g}(G)$, $^4T_{2g}(G)$, $^4A_{1g}(G)$ $^4E_g(G)$, $^2T_{1g}(D)$, $^4E_g(D)$ and $^4T_{1g}(P)$ of regular octahedron. [30]

Optical absorption spectrum of green dolomite recorded in the mull form at RT in the range of 200 - 1200 nm is shown in Fig.3 and that of white dolomite is shown in Fig.4. The green dolomite spectrum shows energies at 13160(760 nm), 13515 (740 nm). 14285 (700 nm), 14995(665 nm) and 19800 (505nm) cm^{-1} in the UV–Vis region whereas white dolomite spectrum shows energies at 12660 (790 nm), 13070 (765 nm), 13425 (745 nm), 22220 (450 nm) cm^{-1} in the UV–Vis region. In green dolomite, the band observed at 13515 with split component on left side at 13160 cm^{-1} is assigned to the transition $^6A_{1g}(S) \rightarrow {}^4T_{1g}(G)$ whereas the band at 14995 cm^{-1} is assigned to $^4T_{2g}(G)$ transition. The third band visible around 19800 cm^{-1} is assigned to $^4A_{1g}(G)$, $^4E_g(G)$ transition. These

bands are characteristic of Fe(III) ion in octahedral symmetry in the mineral. This is also further supported by EPR studies. Using the Tree's polarization term α = 90 cm^{-1} [26], the energy matrices of the d^5 configuration are solved for various B,C and Dq values. The evaluated parameters are presented in Table 2. A comparison is also made between the calculated and observed energies of the bands and these are presented in Table 2. The sharp band observed in green dolomite at 14285 cm^{-1}may due to Mn(II). The very sharp band observed at 13070 cm^{-1} in white dolomite with split component on either side (at 12660 and 13425 cm^{-1} with average of 13043 cm^{-1}) is assigned to the transition $^6A_{1g}(S) \rightarrow {}^4T_{1g}(G)$. Similar assignment is also made in green dolomite. The intensity of the band in white dolomite is large when compared to green dolomite. Further in white dolomite the band visible around 16000 cm^{-1} due to the transition of $^6A_{1g}(S) \rightarrow {}^4T_{2g}(G)$ is not seen. This may be due to low concentration of iron in the mineral. The third band at 22220 cm^{-1} is assigned to $^4A_{1g}(G)$, $^4E_g(G)$ transition. These bands are characteristic of Fe(III) ion in octahedral symmetry in the mineral. This is also further supported by EPR studies. Using the Tree's polarization term α = 90 cm^{-1} [31] the energy matrices of the d^5 configuration are solved for various B,C and Dq values. A comparison is also made between the calculated and observed energies of the bands and these are presented in Table 2. These results are well agree well with the reported values of different dolomite mineral of Indian origin [12].

3.3. Near infrared spectroscopy

Water has three fundamental modes. They are symmetric OH stretch (ν_1), H-O-H bending mode (ν_2) and asymmetric OH stretch (ν_3). In solid phase these appear at 3220 (ν_3), 1620(ν_2) and 3400 (ν_1) cm^{-1} [32]. The shifting of ν_1 and ν_3 towards lower frequency and ν_2 towards higher frequency is due to hydrogen bonding [33]

The 11500 to 5500 cm^{-1} spectral region

Fig. 5 shows near infrared spectrum of dolomite mineral from11500 –5500 cm^{-1} region. The near-IR spectral regions may be conveniently divided as follows: The high wave number region >7500 cm^{-1} : in this region, electronic bands due to characteristic of Fe^{2+} and Fe^{3+} ions are observed. The two bands observed in green dolomite at 9286 and 8581 cm^{-1} are broad and are of very low intensity which are assigned to the two components of the transition $^5T_{2g} \rightarrow {}^5E_g$. This may be due to trace of Fe(II) present in the sample. The average of these bands 8934 cm^{-1} is taken as 10Dq. But in white dolomite no Fe(II) bands are noticed.

The high wave number region between 7200 and 6300 cm^{-1} is attributed to the first overtone of the fundamental hydroxyl stretching mode. The very sharp group of bands at 7127 and split components on either side at 7237 and 7036 cm^{-1} with high intensity are due to $2\nu_3$ the asymmetric OH stretch in the green dolomite. Exactly the similar very sharp group of bands observed at 7154 cm^{-1} with components at 7232, 7173 and 6920 $cm^{-1}$with maximum intensity are assigned to the same $2\nu_3$ asymmetric OH stretch in the white dolomite.

The 5500 to 4000 cm^{-1} spectral region

The spectral region from 5500 to 4000 cm^{-1} is made up of two parts the 4000 – 4500 cm^{-1} region in which OH combination bands are found and 4500 – 5500 cm^{-1} region in which water combination bands are observed. Fig. 6 shows a profile of bands at 4300 cm^{-1} with high intensity and with components on either side at 4397 and 4123 cm^{-1}. These bands in green dolomite are assigned to the water OH combination. In white dolomite, similar bands are observed with less intensity at 4293 cm^{-1} with a shoulder at 4388 cm^{-1}which may be attributed to the water OH combination. The intense band observed at 5083 cm^{-1} in green dolomite is attributed to the water OH overtone. The same band with very low intensity observed at 5078 cm^{-1} in white dolomite is assigned to the water OH overtone. In general the NIR bands observed for white dolomite less intense when compared to green dolomite which indicates that water is more in green dolomite than that present in white dolomite.

Conclusion

1. EPR results indicate that Fe(III) and Mn(II) are present in the mineral in distorted octahedral environment. The g value of 4.34 in green dolomite and that of 4.20 in white dolomite is ascribed to Fe(III). This supports that the sample contains isolated Fe(III) ions in the lattice of the dolomite mineral In both the dolomites, the values of g , A and D in the spectra are g = 1.992 ± 0.015, A = 9.15 ± 0.43 mT and D = 34.45 ± 0.36 mT (white dolomite) and g = 1.993 ± 0.017, A = 9.35 ± 0.43 mT and D = 34.25 ± 0.35 mT. respectively and they are due to Mn(II) indicating of distorted octahedral environment in the mineral. These results suggest that Mn(II) is replaced either Ca and Mg sites. . Also white dolomite shows a free radical at g = 2.1019 which is ascribed to CO_3^{2-} which may be a geological indicator Thus EPR is a very sensitive technique for the magnetic analysis of paramagnetic components in diamagnetic (carbonate) minerals.

2. The optical absorption studies indicate that Fe(III) ion is present in major quantity in both the dolomites whereas Fe(II) is in traces in the green dolomite mineral. These ions are also present in distorted octahedral environment. Green colour of the mineral is due to Fe(II) which is evident from the optical absorption spectrum.

3. Near-infrared spectrum is due to overtones and combinations of water molecules. Also green dolomite sample contains more lattice water than the white dolomite mineral.

Acknowledgements

The authors wish to express their sincere thanks to Prof. P.S.Rao, Dept of Chemistry, Pondicherry University, Puducherry, India for providing EPR instrumental facility.

References

1. www.minerals-n-more.com "The Mineral Dolomite"
2. www.galleries.com "The Dolomite group of Minerals".
3. R. J.Reeder, W.A.Dollase, Am.Miner.**74** (1989) 1159.
4. R. J.Reeder and H.R.Wenk, Am.Miner. **68** (1983) 769.
5. J.W.Anthony, R.A.Bideaux, K.W.Bladh and N.C.Nichols, "Hand Book of Mineralogy Volume V", Mineral Data Publishing , Tucson, AZ,813 (2003) pp191.
6. W.A. Dollase and R.J.Reeder, Am.Miner.**71** (1986) 163.
7. D.E.Miser,J.Steven Swinnea, Hugo Steinfink, Am.Miner. **72** (1987) 188.
8. F.Prissok and G.Lehmann, Phys. Chem. Minerals. **13** (1986) 331.
9 J.Granwehr, P.G.Weidler and A.U.Gehring, Am.Miner. **89** (2004) 785.
10. N.P.Crook, S.R. Hoon, K.G.Taylor and C.T. Perry, Geophysical Journal International, **149** (2002) 328.
11. R.W.A. Franco, F.Pelegrini and A.M. Rossi, Phys.Chem. Minerals, **30** (2003) 39.
12. S.Gunasekaran and G. Anbalagan, Spect. Chim. Acta A, **69** (2008) 383.
13. M. Symons, "Chemical & Biological Aspects of Electron Spin Resonance Spectroscopy", John Wiley & Sons, New York (1978.).
14 De Vos, D.E., B.M. Weckhuysen, and T. Bein., J. Am. Chem. Soc. **118** (1996) 9615
15. The Good Earth, Udaipur, Rajasthan, India. "thegoodearth.co.in".
16. Famous Minerals and Chemicals Private Limited,
17. Mineral data Publishing Version I, © 2001-2005.
18. S..J.Hartan, T.M.Laue, N.D.Chasteen, J.Biol.Chem.**276** (2001) 4461.
19. A. .Abragam, B.Bleancy, "Electron Paramagnetic Resonance of Transtion Ions", Oxford University Press, (1970) p187
20. B. Bleancy, R.S.Rubins, Proc. Phys. Soc. **77** (1961) 103
21. J.M. Nedelec, M.Bouazaoui, S. Turrell, Phys.Chem. Glasses, **40** (1999) 264
22 S. Lakshmi Reddy, N.C. Gangi Reddy, G. Siva Reddy,B. Jagannatha Reddy, Ray L. Frost, Spec.Chim Acta **65** (2006) 684 .
23 S.Lakshmi Reddy, K.N.M.Reddy, G.Siva Reddy, B.J.Reddy, R.L.Frost and Tamio Endo, Spec.Chim Acta (2008) (in press)
24 C.P.Lakshmi Prasuna, K.V.Narasimhulu, N.O.Gopal, J.Lakshmana Rao, T.V.R.K.Rao, Spec. Chim. Acta **60** (2004) 2305.
25. P.Schindler, Am. Miner. **55**,1889 (1970).
26 O.Matumura, J.Phys.Soc.Japan, **14** (1959) 108.
27 E. Simanck, K.A. Muller, J. Phys. Chem. Solids **31** (1970) 1027.
28 A.M.F. Benial, V.Ramakrishnan, R.Murugesan, Spec. Chim Acta A **55** (1999) 2573.
29 V. Wieringen, Discuss. Faraday Soc. **19** (1955) 118.
30 J.Wang, S.Wang and Q Su, J.Solid State Chem. **177** (2004) 895.
31 W.Low and G. Losengasten, J. Mol. Spectroscopy, **12**, (1964) 319.
32 K.Nakamoto " Infrared Spectra of Inorganic and Coordination Compounds", Wiley, New York (1970)
33 G.R. Hunt and J.W. Saliesbury, Mod. Geol, **1** (1970) 283.

Table 1

Chemical composition of dolomite

Component	Per centage		
	1	2	3
$CaCO_3$	53.6	56.6	
$MgCO_3$	42.0	43.0	
CaO	31.7	31.7	31.27
MgO	20.5	20.5	21.12
Fe_2O_3	0.30	0.30	
SiO_2	5.50	1.50	0.12
Al_2O_3	0.50	0.50	
FeO			0.022

1. The Good Earth Udaipur, Rajasthan, India.
2. Famous Minerals &Chemicals Private Limited.
3. Haley, Ontario, Canada, Mineral data publishing version I, 2001-2005.

Table 2

Band headed data with assignments for Fe(III) in natural dolomite mineral .

Dolomite green Dq = 900, B = 605 C= 2600 cm^{-1} α = 90 cm^{-1}			Dolomite white Dq = 900, B = 600 C= 2600 cm^{-1} α = 90 cm^{-1}			Transition from $^6A_{1g}$
Wave length (nm)	Wave number (cm^{-1})		Wave length (nm)	Wave number (cm^{-1})		
	Observed	Calculated		Observed	Calculated	
			790	12660		
760	13160	13161	765	13070	13087	
740	13515		745	13425		$^4T_{1g}(G)$
700	14285		---	---		
665	14995	16951	---	---	16852	$^4T_{2g}(G)$
505	19800	20813	450	22220	20739	$^4E_g(G)$ $^4A_{1g}(G)$

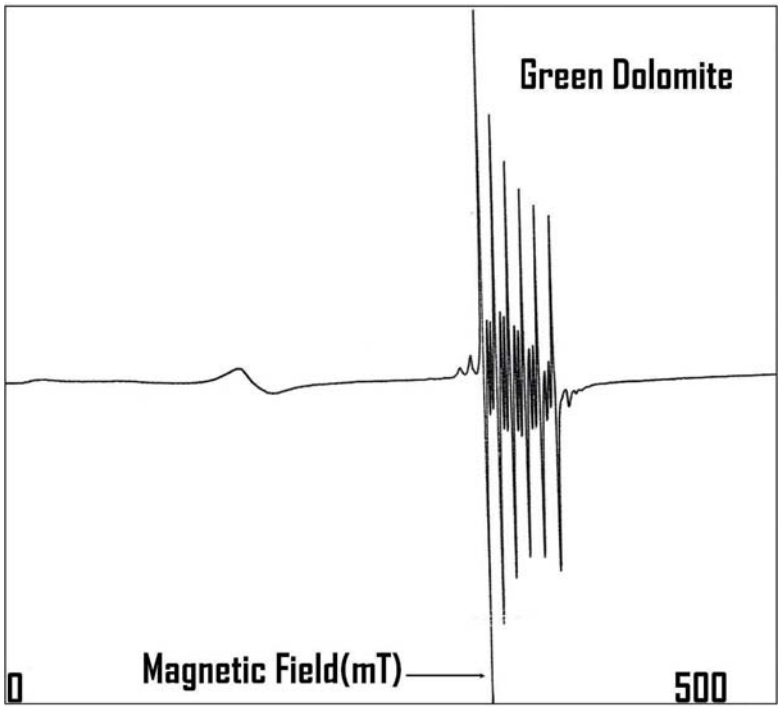

Fig.1(a) EPR spectrum of green dolomite at RT(ν = 9.39219GHz)

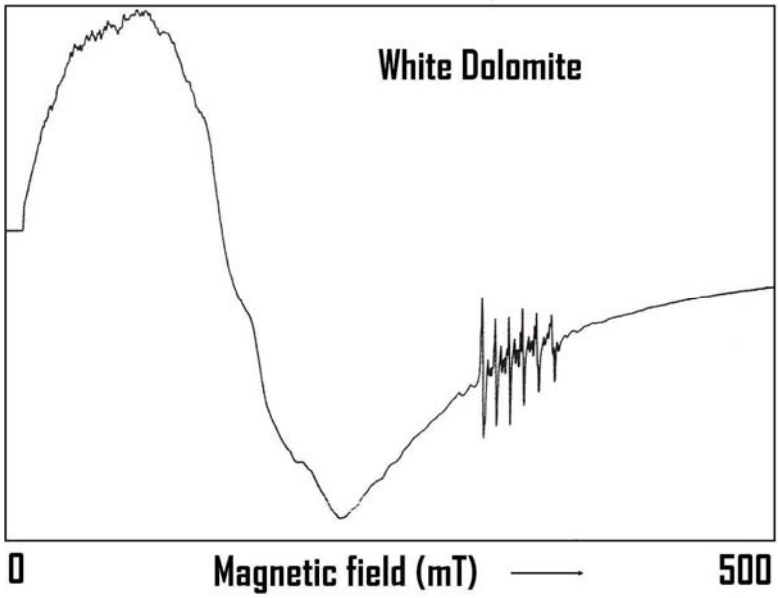

Fig.1(b) EPR spectrum of white dolomite at RT (ν = 9.39208GHz)

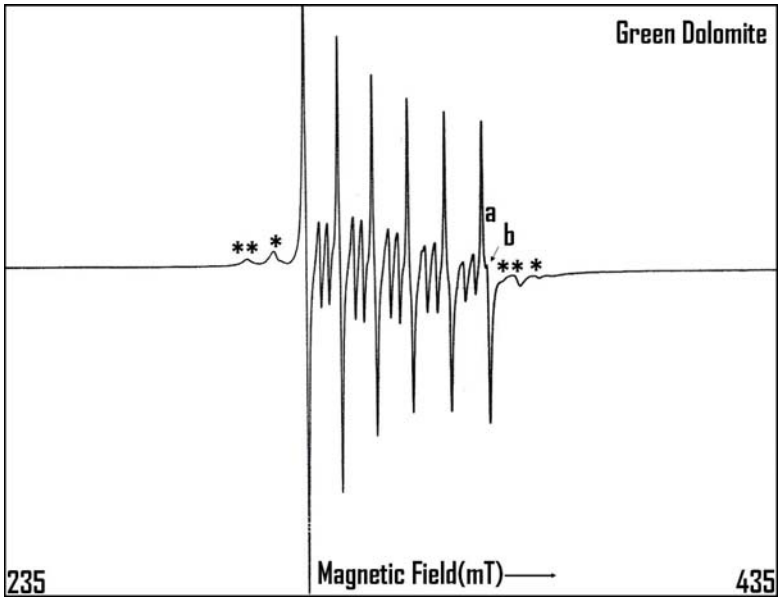

Fig 2(a).Expanded form of EPR Spectrum of green Dolomite at RT(ν = 9.39128GHz)

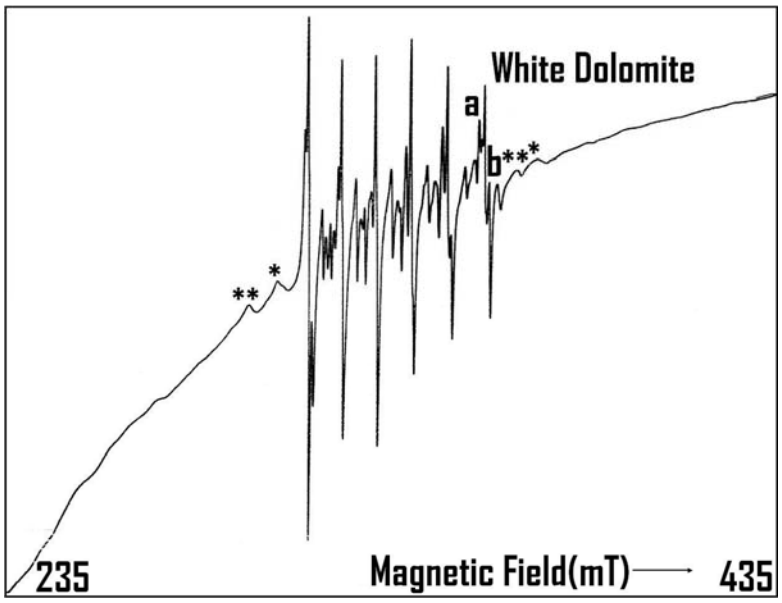

Fig 2(b).Expanded form of EPR Spectrum of white Dolomite at RT(ν = 9.39183GHz)

Fig.3

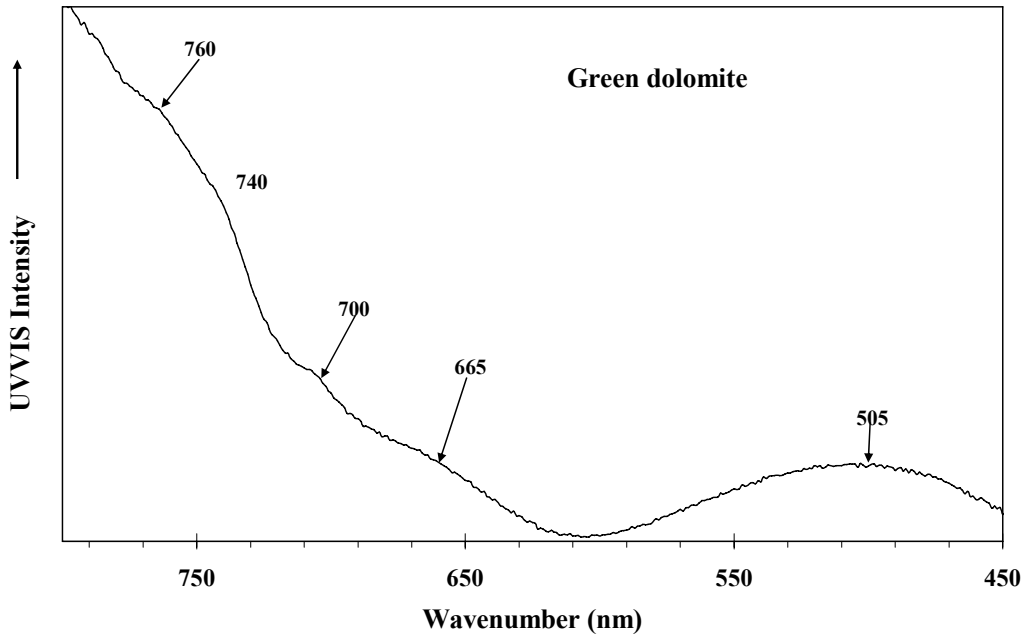

Fig. 3. Optical absorption spectrum of green dolomite at room temperature

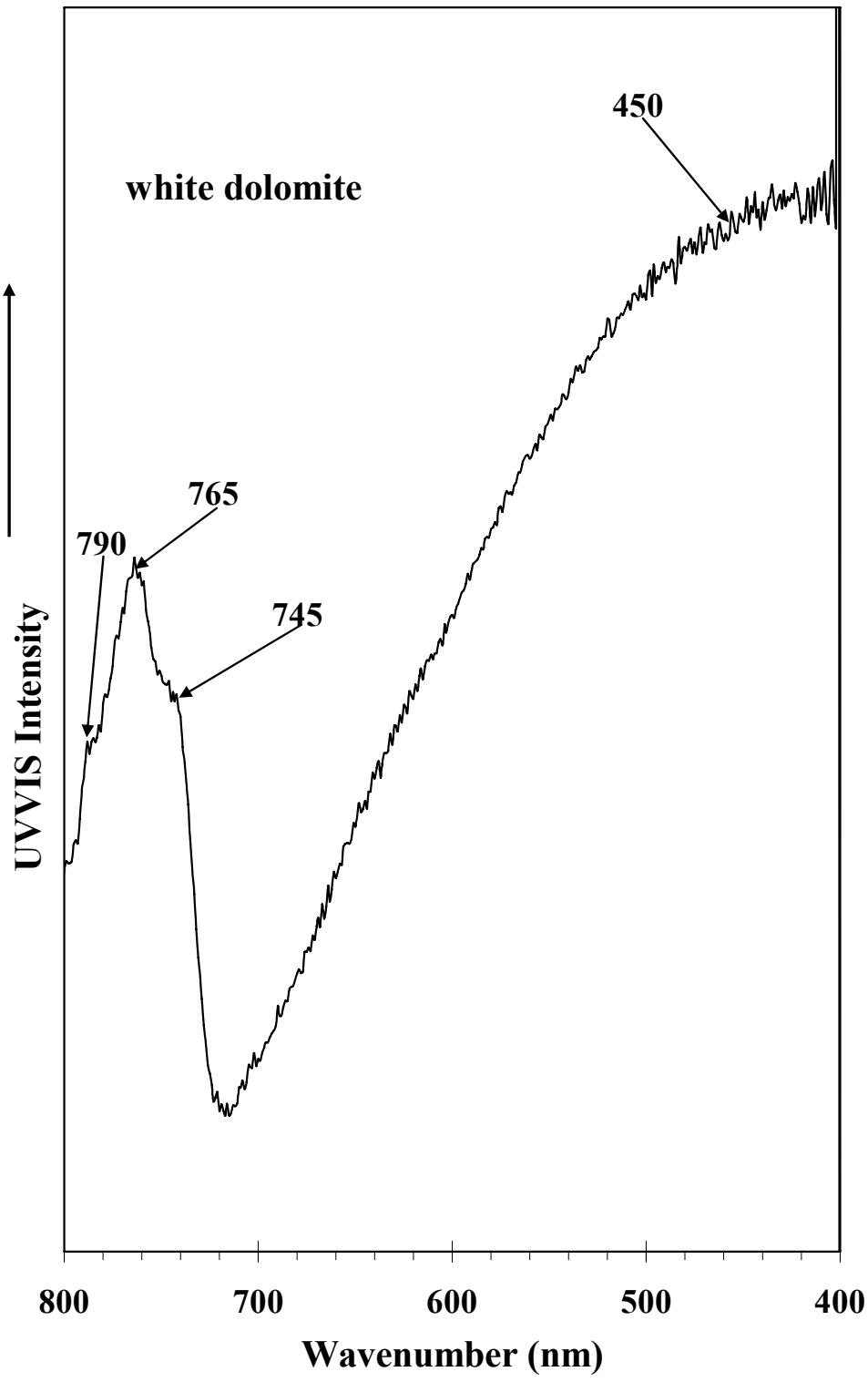

Fig. 4. Optical absorption spectrum of white dolomite at room temperature

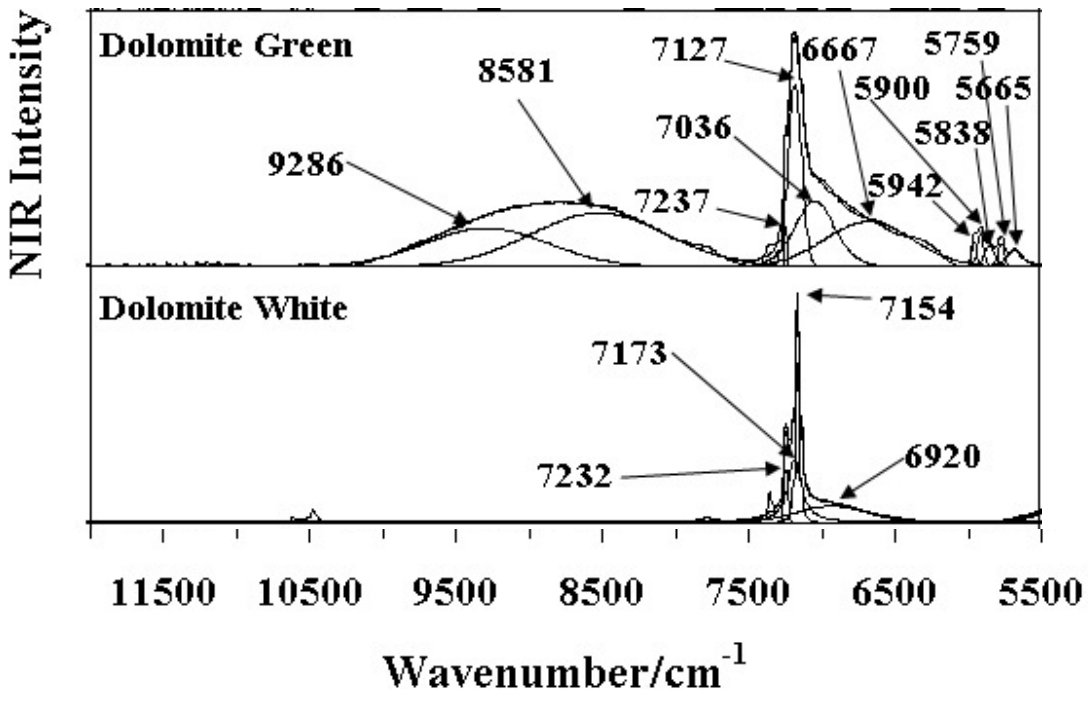

Fig. 5. NIR spectrum of dolomite at room temperature from 11000- 5500 cm^{-1}

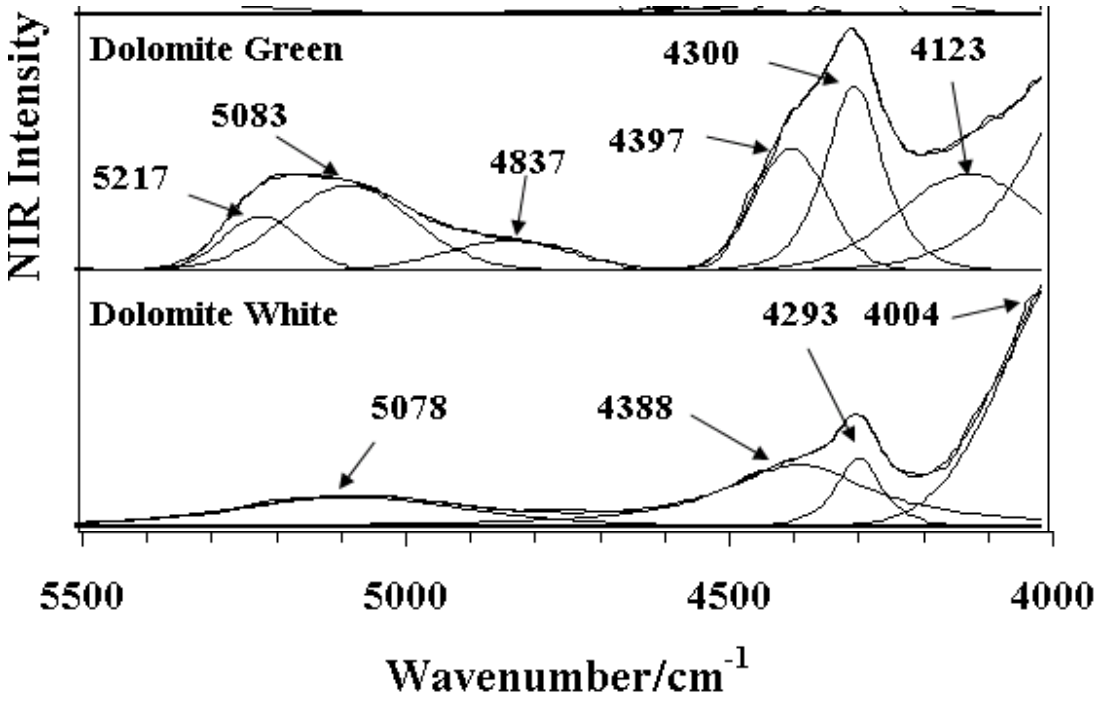

Fig. 6. NIR spectrum of dolomite at room temperature from 5500- 4000 cm^{-1}.